Journal of Medicinal Chemistry

pubs.acs.org/jmc

Article

Novel Cephalosporin Conjugates Display Potent and Selective Inhibition of Imipenemase-Type Metallo-β-Lactamases

Kamaleddin H. M. E. Tehrani, Nicola Wade, Vida Mashayekhi, Nora C. Brüchle, Willem Jespers, Koen Voskuil, Diego Pesce, Matthijs J. van Haren, Gerard J. P. van Westen, and Nathaniel I. Martin*

Cite This: J. Med. Chem. 2021, 64, 9141−9151

Read Online

ACCESS | Metrics & More | Article Recommendations | Supporting Information

ABSTRACT: In an attempt to exploit the hydrolytic mechanism by which β-lactamases degrade cephalosporins, we designed and synthesized a series of novel cephalosporin prodrugs aimed at delivering thiol-based inhibitors of metallo-β-lactamases (MBLs) in a spatiotemporally controlled fashion. While enzymatic hydrolysis of the β-lactam ring was observed, it was not accompanied by inhibitor release. Nonetheless, the cephalosporin prodrugs, especially thiomandelic acid conjugate (**8**), demonstrated potent inhibition of IMP-type MBLs. In addition, conjugate **8** was also found to greatly reduce the minimum inhibitory concentration of meropenem against IMP-producing bacteria. The results of kinetic experiments indicate that these prodrugs inhibit IMP-type MBLs by acting as slowly turned-over substrates. Structure−activity relationship studies revealed that both phenyl and carboxyl moieties of **8** are crucial for its potency. Furthermore, modeling studies indicate that productive interactions of the thiomandelic acid moiety of **8** with Trp28 within the IMP active site may contribute to its potency and selectivity.

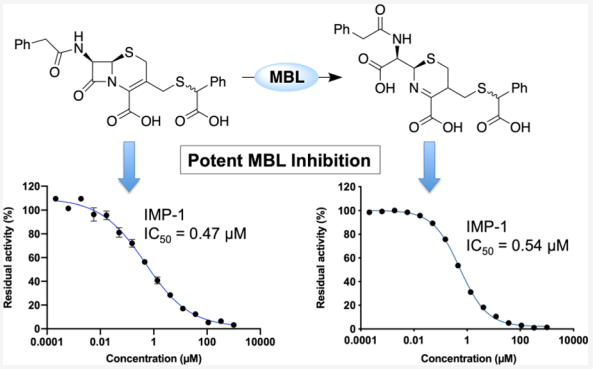

INTRODUCTION

Despite the growing threat of β-lactam resistance caused by metallo-β-lactamases (MBLs), there are no approved drugs on the market that target this class of enzymes. Unlike serine-β-lactamases, MBLs are metalloenzymes containing one or two zinc ions in their active site. An activated water molecule, coordinated by these zinc ions, in turn acts as the nucleophile in the hydrolysis of all classes of β-lactams (except monobactams).[1−3] MBLs of particular clinical significance are the New Delhi metallo-β-lactamase (NDM), Verona integron-encoded metallo-β-lactamase (VIM), and imipenemase (IMP) families, all of which possess broad spectrum β-lactamase activity.[4] The previously reported inhibitors of MBLs have been the subject of several comprehensive review articles.[5−8] Indeed, a wide range of compounds have been reported as MBL inhibitors with the majority acting by either sequestering zinc and/or by forming a ternary complex with metalloenzyme.[9,10]

Previously, we described the *in vitro* ability of a selected group of thiols (**1**−**3**, Figure 1A) to inhibit MBLs and in doing so resensitize a panel of MBL-producing clinical isolates to meropenem, a potent carbapenem antibiotic.[11] Our earlier studies used isothermal titration calorimetry (ITC) to demonstrate that thiols **1** and **2** bind zinc with K_d values of 10 and 20 μM, respectively. However, as we also demonstrated, these thiol-containing compounds are prone to rapid oxidation to their corresponding disulfides, leading to the loss of zinc-binding affinity, MBL inhibition, and synergistic activity.[11] Recently, we reported a cephalosporin prodrug approach to selectively enable the release of strong zinc-chelating small molecules upon hydrolysis by MBLs.[12] In doing so, we identified inhibitors with potent activity against NDM- and VIM-type MBLs. In the present study, we aimed to apply a similar design strategy employing thiol-based MBL inhibitors **1**−**3**. As illustrated in Figure 1B, the prodrugs consist of a cephalosporin core with the thiol-based MBL inhibitors linked at the 3-position. The hydrolytic action of MBLs upon such conjugates was envisioned to result in a cascade reaction, ultimately leading to release of the inhibitor with both spatial and temporal control. We hypothesized that in the case of thiol-based inhibitors **1**−**3**, this prodrug strategy could be effective by addressing not only the selectivity but also their poor stability stemming from their rapid oxidation. Here, we describe the preparation of cephalosporin−thiol conjugates **6** and **8**−**10** and evaluation of their performance as

Received: February 28, 2021
Published: June 29, 2021

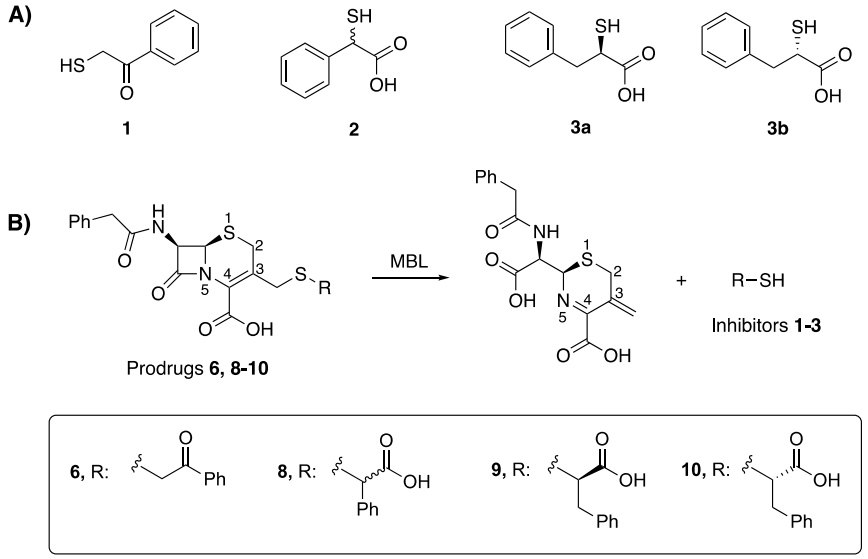

Figure 1. (A) Previously reported thiols as MBL inhibitors. (B) Cephalosporin prodrugs of the thiols **1**−**3** and their related structural analogues.

Scheme 1. Chemical Route to the Cephalosporin Conjugates[a]

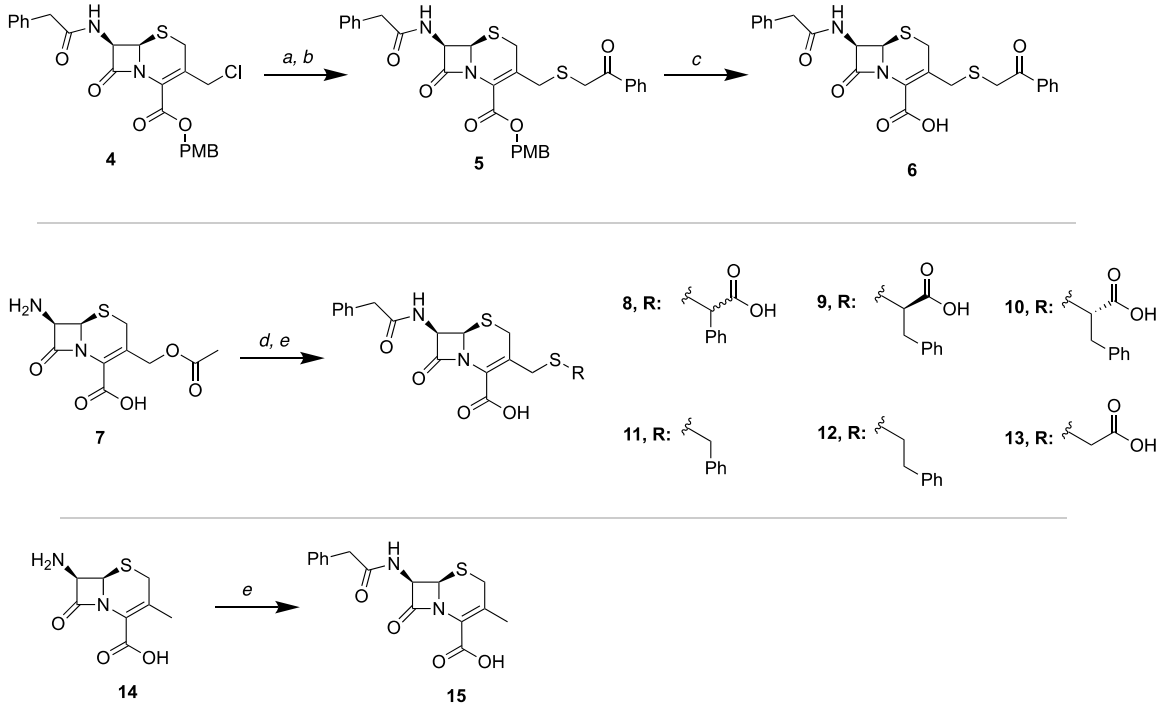

[a]Reagents and Conditions: (a) NaI, DMF, r.t., 30 min; (b) $NaHCO_3$, **1**, r.t., 20 h; (c) TFA, Anisole, 0 °C, 1 h; (d) $BF_3{\cdot}OEt_2$, Thiols, acetonitrile, 45 °C, 2 h; (e) phenylacetyl chloride, saturated $NaHCO_3$ solution, acetone, r.t., 20 h.

MBL-inhibitor prodrugs capable of resensitizing MBL-expressing strains to β-lactam antibiotics.

RESULTS AND DISCUSSION

The cephalosporin−thiol conjugates were synthesized using two different routes (Scheme 1). Thioalkylation of mercaptoacetophenone with the chloromethyl cephalosporin "GCLE" (**4**), a common intermediate used in the industrial synthesis of cephalosporin antibiotics, yielded intermediate **5**, followed by deprotection with trifluoroacetic acid (TFA) to yield compound **6**. Alternatively, compounds **8**−**13** were prepared via the BF_3-promoted substitution of 7-aminocephalosporanic acid (7-ACA, **7**) with the corresponding thiols, followed by acylation of the 7-amino group (see the Experimental Section for detailed procedures). Notably, conjugate **8** was prepared as a diastereomeric mixture, given the stereochemical instability of the corresponding thiomandelic acid building block **2**.[13] Compounds **11**−**13** and **15** were designed and synthesized for the purpose of structure−activity relationship evaluation of the thiol conjugates **6** and **8**−**10**.

To assess the zinc-binding properties of the cephalosporin−thiol conjugates, ITC binding studies were performed, which revealed no appreciable binding interaction with zinc (data not shown). This is in contrast with the thiols **1**−**3** themselves,

https://doi.org/10.1021/acs.jmedchem.1c00362
J. Med. Chem. 2021, 64, 9141−9151

Table 1. MIC of Meropenem in Combination with the Cephalosporin Conjugates Tested at Multiple Concentrations against Four Clinical Isolates

		meropenem MIC (μg/mL)			
compound	concentration (μg/mL)	*E. cloacae* (IMP-1)	*K. pneumoniae* (IMP-28)	*E. coli* (VIM-2)	*E. coli* (NDM-1)
6	0	16	4	8	32
	32	8 (2)[a]	1 (4)	8 (1)	16 (2)
	64	8 (2)	0.5 (8)	4 (2)	8 (4)
	128	4 (4)	0.25 (16)	4 (2)	8 (4)
8	0	32	4	8	32
	32	1 (32)	≤0.063 (≥64)	4 (2)	16 (2)
	64	0.5 (64)	≤0.063 (≥64)	2 (4)	16 (2)
	128	0.5 (64)	≤0.063 (≥64)	1 (8)	8 (4)
9	0	32	4	8	32
	32	1 (32)	≤0.063 (≥64)	4 (2)	16 (2)
	64	1 (32)	≤0.063 (≥64)	4 (2)	8 (4)
	128	0.5 (64)	≤0.063 (≥64)	2 (4)	8 (4)
10	0	16	4	8	64
	32	8 (2)	1 (4)	8 (1)	32 (2)
	64	8 (2)	0.5 (8)	8 (1)	32 (2)
	128	4 (4)	0.25 (16)	4 (2)	16 (4)
11	0	32	2	4	32
	32	8 (4)	0.5 (4)	2 (2)	16 (2)
	64	8 (4)	0.25 (8)	2 (2)	16 (2)
	128	4 (8)	0.25 (8)	1 (4)	16 (2)
12	0	16	4	8	64
	32	8 (2)	0.5 (8)	8 (1)	32 (2)
	64	8 (2)	0.25 (16)	4 (2)	16 (4)
	128	8 (2)	0.25 (16)	4 (2)	16 (4)
13	0	16	2	4	32
	32	8 (2)	0.25 (8)	2 (2)	16 (2)
	64	8 (2)	0.25 (8)	2 (2)	16 (2)
	128	4 (4)	0.125 (16)	1 (4)	8 (4)
15	0	16	2	4	32
	32	16 (1)	1 (2)	2 (2)	16 (2)
	64	16 (1)	0.5 (4)	2 (2)	16 (2)
	128	16 (1)	0.25 (8)	1 (4)	16 (2)
DPA[b]	0	32	2	4	32
	32	16 (2)	0.125 (16)	≤0.063 (≥64)	0.5 (64)
	64	1 (32)	≤0.031 (≥64)	≤0.063 (≥64)	0.5 (64)
	128	0.25 (128)	≤0.031 (≥64)	≤0.063 (≥64)	≤0.5 (≥64)

[a]Fold reduction of MIC shown in brackets. [b]Dipicolinic acid.

which were previously shown to be strong zinc-binders with low μM K_d values.[11] In addition, stability analyses were performed to test whether inhibitor release occurred spontaneously. Following overnight incubation in Mueller–Hinton broth (MHB), HPLC analysis of the conjugates **6** and **8**–**10** showed that all demonstrated good stability (>95% intact after 15 h, Table S1).

The compounds were tested for their performance against a panel of MBL-producing clinical isolates. After it was found that the cephalosporin conjugates do not inhibit bacterial growth at concentrations up to 128 μg/mL, their ability to restore the antibacterial activity of meropenem was tested. The results showed that compound **8** and **9** were potent synergists, lowering the minimum inhibitory concentration (MIC) of meropenem against IMP-producing isolates most effectively (Table 1).

Encouraged by the promising results against the MBL-producing clinical isolates, we tested the ability of the conjugates to inhibit purified IMP-1, IMP-28, VIM-2, and NDM-1 enzymes. The biochemical assay used for these studies employed the chromogenic cephalosporin nitrocefin as the substrate.[8] The IC_{50} data thus obtained revealed conjugates **8** and **9** to be particularly potent and selective IMP inhibitors (Table 2). These findings are consistent with the trends observed in the bacterial growth inhibition synergy assays, where strains possessing IMP-type enzymes were also most sensitive to meropenem when coadministered with conjugates **8** and **9**. Sequence alignment of IMP-1 and IMP-28 does not reveal any differences in the amino acids comprising the active sites (Table S2). Overall, the two enzymes share a high sequence identity (92.28%). Among the few amino acid differences outside the active site, the His306Gln mutation has been proposed to be responsible for the overall decreased hydrolytic efficiency of IMP-28 compared to IMP-1.[14] However, as far as the inhibitory profile of the cephalosporins evaluated in this study is concerned, the two enzymes showed similar performance.

To investigate the mechanism of inhibition, and more specifically to assess release of the thiol inhibitors, the most potent cephalosporin conjugates **8** and **9** were incubated with

https://doi.org/10.1021/acs.jmedchem.1c00362
J. Med. Chem. 2021, 64, 9141−9151

Table 2. IC_{50} (μM) of Cephalosporin Conjugates Reported as Mean ± SD[a]

compound	IMP-1	IMP-28	NDM-1	VIM-2
6	3.3 ± 0.2	14 ± 1	77 ± 12	76 ± 11
8	0.47 ± 0.08	0.46 ± 0.04	>100	10 ± 0.5
9	4.7 ± 0.4	1.1 ± 0.2	94 ± 0.2	16 ± 1
10	48 ± 0.7	30 ± 9	51 ± 1	19 ± 1
11	43 ± 3	45 ± 5	>100	73 ± 0.1
12	2.2 ± 0.4	4.3 ± 0.8	>100	49 ± 3
13	>100	>100	72 ± 2	53 ± 12
15	>100	>100	>100	57 ± 9
DPA	29 ± 0.5	29 ± 5	10 ± 0.1	10 ± 0.8

[a]Assay used nitrocefin used as the chromogenic substrate. A detailed description of the assay can be found in the Experimental Section.

IMP-28 and analyzed using ^{1}H NMR and LC−MS techniques. It has been shown previously by our group and others that the molecular mechanism of cephalosporin hydrolysis can be probed *in situ* using NMR techniques.[12,15−17] In the present study, we used the commercially available 7-phenylacetylamide derivative of 7-ACA (compound **16**, Figure 2A) as a positive control. After incubating compound **16** with IMP-28, the rapid appearance of vinylic protons corresponding to the elimination product was detected at *ca.* 5.50 ppm (Figure 2A). However, when **8** and **9** were subjected to the same experiment, these vinylic signals were not detected (Figure 2B), suggesting that the thiols at the 3-position were not released. The results of these ^{1}H NMR studies were further corroborated by LC−MS analyses of the enzymatic hydrolysis products of **8** and **9**, which revealed the hydrolyzed β-lactam compounds **8H** and **9H** as the only detectable products (Figure 2C, see Supporting Information Figures S2−S4 and S7 for complete NMR and LC−MS data). Given that previous studies published by our group and others have detected the release of aromatic thiols as leaving groups after incubation with MBLs,[12,18] we ascribe the observed lack of inhibitor release in our study to the poor leaving group quality of the aliphatic thiols we used.

The finding that compounds **8** and **9** demonstrate potent inhibition of IMP-28 despite not releasing the corresponding zinc-binding thiol inhibitors upon MBL-mediated β-lactam hydrolysis was surprising. To better understand the mechanism of inhibition of these cephalosporin conjugates, we next determined the kinetic parameters of the hydrolysis of the cephalosporin conjugates using purified MBL enzymes. In addition, we evaluated the MBL-inhibitory activity of the partial hydrolysis products **8H** and **9H**. The kinetic analysis of the hydrolysis of the cephalosporins by IMP-28, NDM-1, and VIM-2 provided valuable insights into the IMP-28 selectivity and inhibitory potency observed for **8** and **9**. These analyses

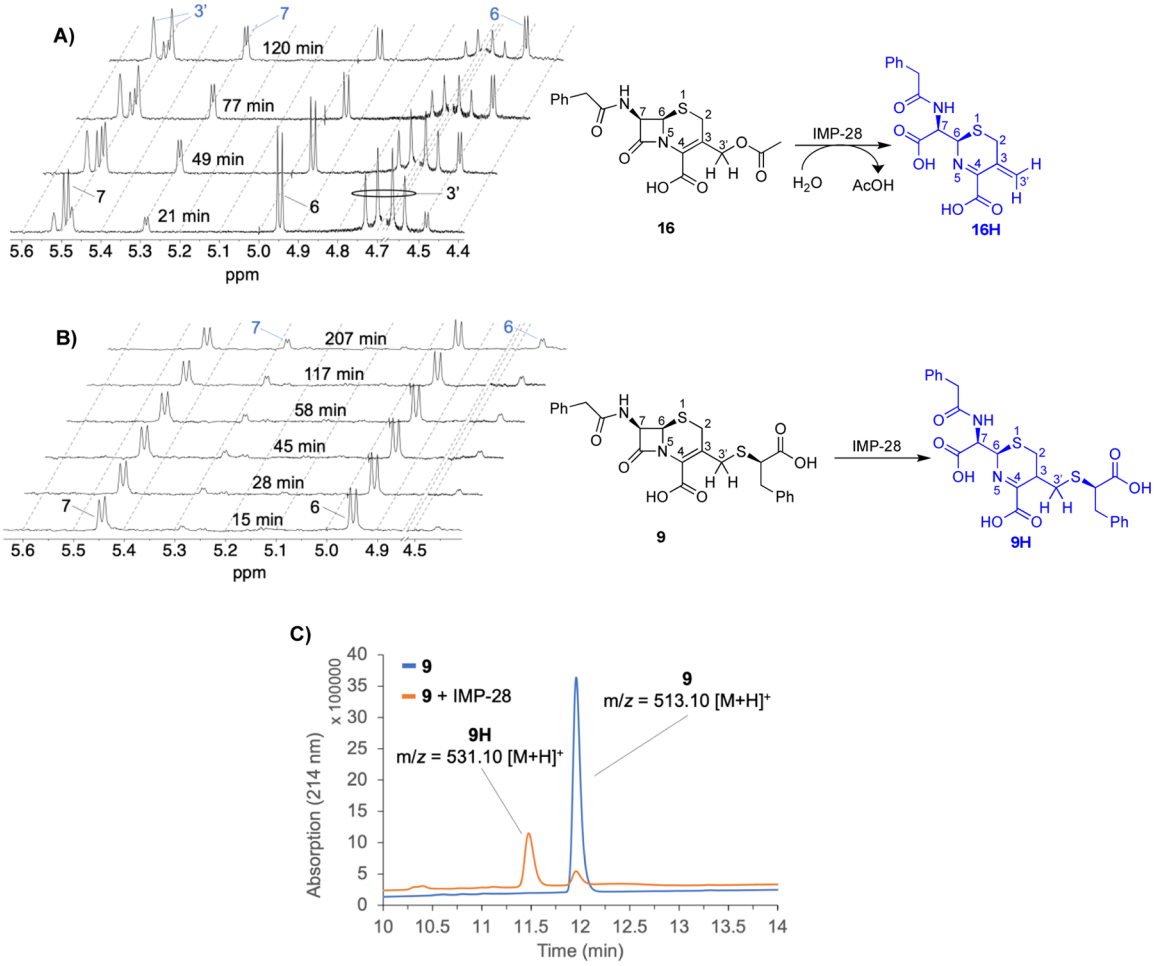

Figure 2. (A) Enzymatic degradation of **16** showing the growth of the signals corresponding to the vinylic protons of **16H** resonating as two singlets *ca.* 5.5 ppm. (B) Enzymatic degradation of **9** instead leads to **9H**. For the purpose of clarity, the segment corresponding to water signal has been omitted from the NMR spectra. (C) LC−MS analysis of IMP-28-mediated degradation of **9**, confirms the exclusive formation of **9H**.

https://doi.org/10.1021/acs.jmedchem.1c00362
J. Med. Chem. 2021, 64, 9141−9151

showed that IMP-28 has the lowest catalytic efficiency for **8** and **9** among the tested cephalosporins (see Table 3 for relative k_{cat}/K_M data). Comparison with the other major MBL families also revealed that **8** and **9** were hydrolyzed more efficiently by NDM-1 and VIM-2 than by IMP-28. We also determined the IC_{50} of **8** and **9** against IMP-28 following different incubation times (0−60 min). As shown in Figure S5, maximum increase in potency is observed after 15 min incubation, after which the potency stabilizes. This might indicate that either active site recognition does not occur instantly or that over 15 min time course, the more potent hydrolysis products (**8H** and **9H**) are produced, which might be responsible for the sub-micromolar inhibition. These findings indicate that conjugates **8** and **9** inhibit IMP-28 either by acting as slowly turned-over substrates and/or that the hydrolyzed products **8H** and **9H** are more tightly bound within the IMP active site than either the NDM or VIM active sites.

Table 3. Michaelis−Menten Parameters Determined for the Cephalosporin Conjugates as Substrates of IMP-28, VIM-2, and NDM-1.[a,b]

enzyme	substrate	K_M (μM)	k_{cat} (s^{-1})	kcat/K_M ($\mu M^{-1}\cdot s^{-1}$)	relative kcat/K_M
NDM-1	**8**	14.0 ± 2	13.1	0.936	100
	9	21.2 ± 4	17.4	0.821	88
VIM-2	**8**	8.28 ± 2	4.06	0.490	52
	9	4.30 ± 1	2.35	0.546	58
IMP-28	**8**	129 ± 13	0.386	0.003	0.30
	9	249 ± 7	2.83	0.011	1.2
	10	175 ± 19	41.0	0.234	44
	11	20.5 ± 4	10.8	0.529	56
	12	83.3 ± 16	6.12	0.073	14
	13	219 ± 23	37.0	0.169	18
	15	392 ± 73	23.3	0.059	6.3

[a]Experimental procedure has been described in detail in the Experimental Section. [b]See the Supporting Information for the Michaelis−Menten graphs.

To evaluate the inhibitory activity of the hydrolysis products **8H** and **9H**, the intact conjugates **8** and **9** were first fully hydrolyzed by incubation with NDM-1, as described in the Experimental Section (see Figure S8 for the LC−MS traces). Following hydrolysis, the NDM-1 enzyme was completely removed via spin-filtration, as confirmed by the lack of nitrocefin activity in the filtrate. The partially hydrolyzed **8H** and **9H** were then tested for their capacity to inhibit MBLs.

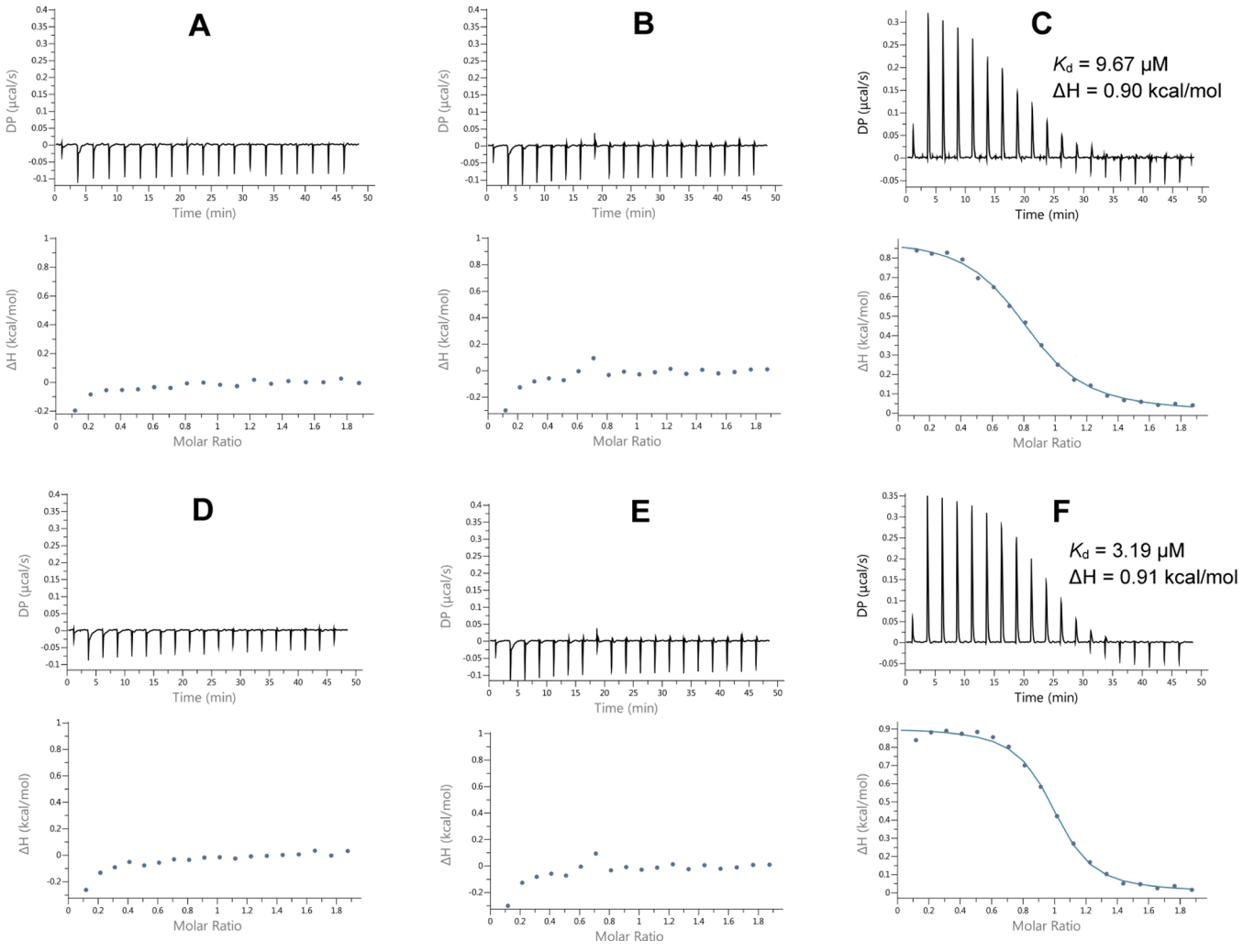

Figure 3. ITC thermograms resulting from titration of $ZnSO_4$ into a solution containing: (A) compound **8**; (B) purified NDM-1; (C) compound **8H**; (D) compound **9**; (E) purified NDM-1; (F) compound **9H**.

https://doi.org/10.1021/acs.jmedchem.1c00362
J. Med. Chem. 2021, 64, 9141−9151

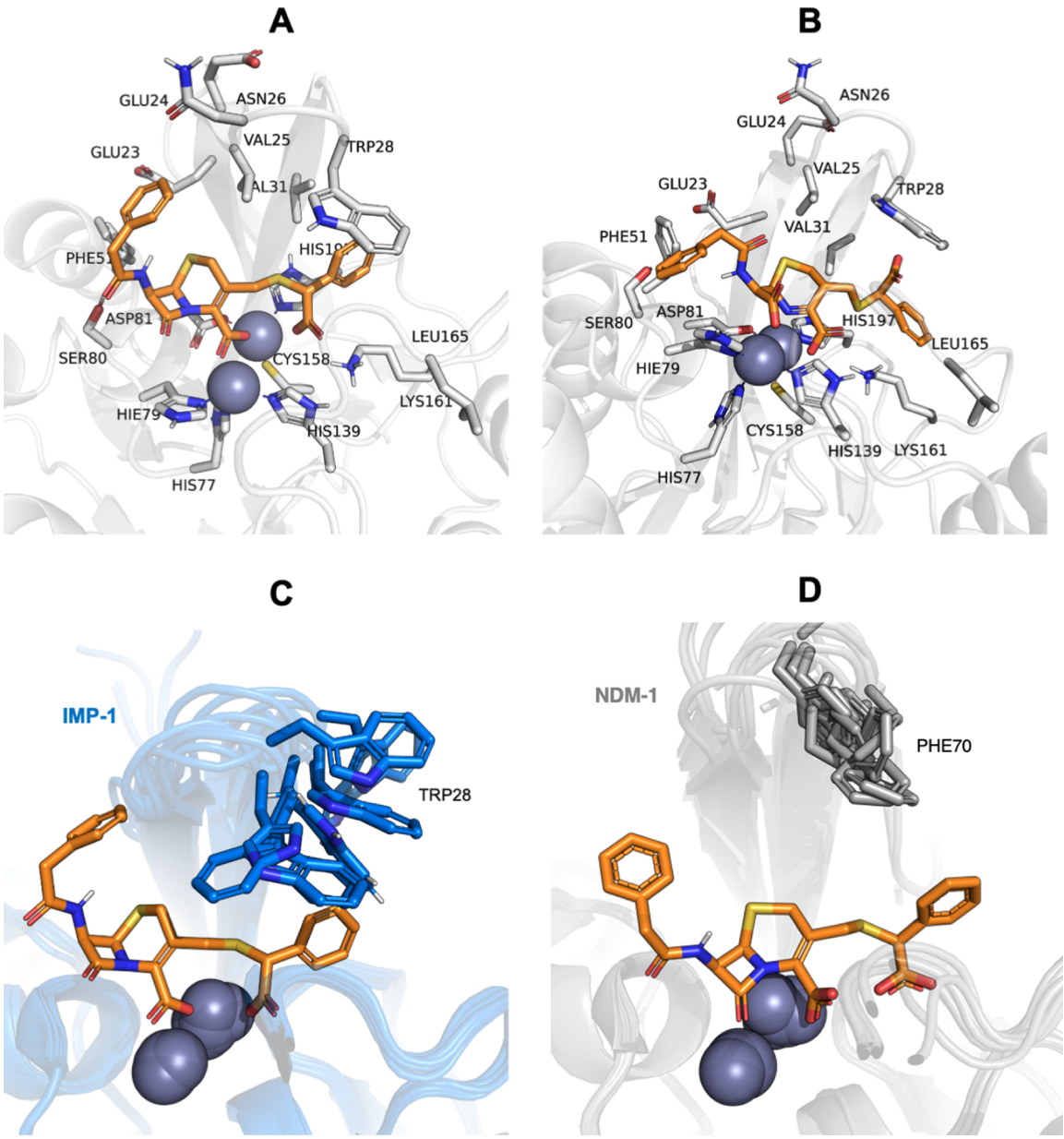

Figure 4. Modeling studies of compound **8** and **8H** docked into the active site of IMP-1 (PDB ID: 1dd6)[19] and NDM-1 (PDB ID: 4RL2).[16] For simplicity, only the diastereomer of **8** containing the *R*-thiomandelic acid moiety has been shown. (A) Compound **8** in the active site of IMP-1. The carboxylates of both the thiomandelic acid moiety and at the cephem C-4 position are predicted to interact with the zinc ions in IMP-1. Also notable is the $\pi-\pi$ interaction of phenyl ring of **8** with Trp28. (B) Compound **8H** in the active site of IMP-1. Compared to **8**, the carboxylate resulting from the β-lactam hydrolysis is predicted to replace the thiomandelic acid carboxylate in coordinating the zinc ions. In addition, the phenyl ring of the thiomandelic acid moiety is extended toward the lipophilic pocket around Leu165. (C) Docking model of compound **8** shown in an ensemble of overlaid X-ray structures of IMP-1. (D) Docking model of compound **8** shown in an ensemble of overlaid X-ray structures of NDM-1.

Interestingly, both hydrolysis products were found to possess potent activity against IMP-1 and IMP-28 with sub-micromolar IC_{50} values (Table S3). In addition, the hydrolysis products **8H** and **9H** were evaluated for their zinc-binding affinity using ITC. When zinc was titrated into the solution of **8** and **9** preincubated with NDM-1 to generate **8H** and **9H** *in situ*, a binding interaction was observed with K_d values of 9.67 and 3.19 μM measured, respectively (Figure 3). By comparison, the intact cephalosporins showed no zinc-binding affinity. This affinity for zinc binding may therefore also contribute to the inhibitory activity of **8H** and **9H**.

The IC_{50} data obtained for the various conjugates prepared also provide some structure–activity insights (Table 2). Specifically, elimination of the carboxylic acid (**11**), phenyl group (**13**), or the entire thiomandelic acid fragment (**15**) causes the activity against IMP-1 and IMP-28 to be decreased by ca. 100-fold, suggesting that the thiomandelic acid fragment introduces productive binding interactions with the IMP active site. Among the derivatives, the moderate synergistic activity of **13** against IMP-28 producing *Klebsiella pneumoniae* could be due to the fact that lower lipophilicity might contribute to improved cellular accumulation of **13**. Also interesting was the observation that compound **9** was ca. 10-fold and 30-fold more

https://doi.org/10.1021/acs.jmedchem.1c00362
J. Med. Chem. 2021, 64, 9141–9151

potent than its diastereomer **10** against IMP-1 and IMP-28, respectively.

In an attempt to provide further insights into the binding mode of the most potent compound (**8**), a computational model was derived based on docking of this compound to the published crystal structure of IMP-1.[19] The docking hypothesis is based on the high resemblance of **8H** to the hydrolysis product of cephalexin, a compound previously cocrystallized with NDM-1.[16] Thus, we overlaid the IMP-1 and NDM-1 structures and used the maximum common substructure (MCS, see the Experimental Section) between **8H** and the hydrolysis product of cephalexin. The resulting docking pose aligned well with **8H**, as well as other representative hydrolysis products presented in this work. Noteworthy is the fact that both diastereomers of **8H**, which could not be separated for the assay, are accommodated in the binding site and in a similar fashion (see Figure S9). We next studied the docking of the parent compound **8**, which revealed some interesting findings in comparison with its hydrolysis product **8H**: in the docking model of compound **8** in IMP-1 (Figure 4A), the zinc ions are anchored by the carboxylate on cephem C-4 together with the carboxylate from the thiomandelic acid moiety. The latter in **8H** (Figure 4B) is replaced by the carboxylate resulting from β-lactam hydrolysis. In NDM-1, however, the carboxylate on cephem C-4 as well as β-lactam carbonyl of **8** are predicted to interact with the zinc centers (see the Supporting Information for supplementary PDB files). This difference in the mode of interaction of **8** with IMP-1 versus NDM-1 may explain the importance of thiomandelic acid carboxylate for the potency of **8** against IMPs. Also notable for **8H** is the way the phenyl group of the thiomandelic acid moiety interacts with the Trp28 and Leu165 residues of IMP-1. The binding mode of **8** suggests that this phenyl group can engage in a $\pi-\pi$ interaction with Trp28 (Figure 4A). Upon hydrolysis to **8H**, however, this phenyl group is predicted to move away from Trp28 and toward Leu165, where it can form hydrophobic interactions in a pocket around that residue (Figure 4B). Another interesting observation that may at least partly explain the selectivity of **8** for IMP versus NDM-type MBLs is a predicted interaction with Trp28. An analysis of all available IMP-1 structures (Figure 4C) indicates that the Trp28 side chain is part of a flexible loop region that can form a cage around the binding site, optimally accommodating compound **8**. Interestingly, in NDM-1 this residue is replaced by Phe70, where it is part of a more flexible region, as observed in the analysis of all X-ray structures for NDM-1 (Figure 4D). These differences may contribute to a mode of binding for compound **8** in the NDM-1 active site that leads to hydrolysis of the β-lactam ring, while in the case of IMP-1, a different binding mode is adopted, leading instead to inhibition. Specifically, the lower flexibility of the L3 loop in IMP-1, and its higher proximity toward the side-chain phenyl of compound **8**, might therefore enforce binding interactions that support the inhibitory activity of compound **8** rather than accelerating its hydrolysis by the enzyme. This might explain the relatively high K_M value of **8** despite its potent inhibitory activity against IMP-1. Molecular dynamics (MD) simulations were also performed showing that the docking poses for each diastereomer of **8** and **8H** were stable along triplicate MD simulations (3×10 ns, see Experimental Section for details).

In recent years, a number of groups have reported attempts at designing inhibitors that offer a higher MBL selectivity than zinc-chelating agents (e.g., DPA and EDTA) can provide. Among them, cyclic boronates represented by taniborbactam,[20] indole carboxylic acids,[21] and the thiazole carboxylic acid ANT431[22,23] hold promise for further clinical development. As recently shown by our group and others, MBLs in the B1 class (NDM, VIM, and IMP) exhibit different inhibitory profiles when tested against known MBL inhibitors *in vitro*.[24,25] Clearly, the development of selective and broad-spectrum MBL inhibitors is not an easy task. In the case of ANT431 and its related analogues, for instance, there is a promising inhibitory activity against NDM-1 (IC_{50} = 2.67 μM) and VIM-2 (IC_{50} = 6.7 μM). However, VIM-1 and IMP-1 remain resistant. At this time, taniborbactam is the only β-lactamase inhibitor in clinical trials that also exhibits activity against MBLs (currently phase III, ClinicalTrials.gov Identifier: NCT03840148).[20] The unique cyclic boronate pharmacophore[26] of taniborbactam allows it to mimic the transition state of the β-lactam hydrolysis reaction mediated by both serine and MBLs. This explains the potent and broad-spectrum activity of taniborbactam against β-lactamases of all four Ambler classes (A–D). Interestingly, however, a closer look at the MBL inhibition profile of taniborbactam and its related analogues shows weak inhibition of the IMP family despite the sub-micromolar IC_{50} against NDM-1 and VIM-2.[20] Notably, a recently published patent filing describes a library of indole-2-carboxylic acids some of which demonstrate sub-micromolar IC_{50} values against IMP-1, NDM-1, and VIM-2, as well as promising synergistic activity in combination with meropenem.[21] Interestingly, compound **8** described in our present study demonstrates potent and selective inhibition of IMP-type MBLs with comparatively little activity against NDM- and VIM-type enzymes. In the absence of structural insights by X-ray crystallography, computational approaches offer a means of rationalizing this activity. In addition, the availability of crystal structures for other MBLs from the B2 (e.g., CphA[27]) and B3 (e.g., L1[28] and AIM-1[29]) classes also points to the opportunity to conduct similar *in silico* studies aimed at designing inhibitors that also cover such enzymes.

CONCLUSIONS

We here describe a series of cephalosporin-based MBL inhibitor prodrugs designed to release zinc-chelating small-molecule thiols upon MBL-mediated hydrolysis. Notably, while displaying potent inhibition of IMP-type MBLs, these conjugates did not function as mechanistically predicted. While MBL-mediated hydrolysis was observed, the release of the small-molecule thiol fragments did not spontaneously occur for the conjugates included in this study. This lack of release is presumably due to the pK_a of the corresponding thiols not being low enough to enable them to behave as leaving groups. Nonetheless, the finding that the cephalosporin conjugates (**6**, **8**, and **9**) selectively inhibit IMP enzymes is notable. Based on kinetic analyses, the most potent conjugates **8** and **9** were shown to be slowly turned-over substrates of IMP-28. In addition, the hydrolysis products **8H** and **9H** were found to be IMP-selective inhibitors. Our findings suggest that the IMP inhibition observed with compounds **8** and **9** may be due to a combination of effects, whereby the slowly turned-over substrate and the resulting hydrolysis product both contribute to enzyme inhibition. Furthermore, modeling studies indicate that the interaction of **8**/**8H** and **9**/**9H** with the IMP active site residues Trp28 and Leu165 may contribute to the observed potency and IMP selectivity. These findings provide new insights expected to be of value in future efforts aimed at

https://doi.org/10.1021/acs.jmedchem.1c00362
J. Med. Chem. 2021, 64, 9141–9151

improving the potency, as well as broadening the spectrum of inhibition, of cephalosporin-based MBL inhibitor prodrugs.

EXPERIMENTAL SECTION

General. Compound **4** (GCLE), 7-ACA (**7**), and 7-ADCA (**14**) were purchased from Combi-Blocks (US) and nitrocefin from Cayman Chemical. The preparation of thiols **1**−**3** was performed as previously described.[11] Compound **16** was synthesized via the acylation of 7-ACA following a previously reported procedure.[30] Proton and carbon nuclear magnetic resonance spectra were recorded on an AV400 NMR spectrometer (Bruker), and samples were dissolved in $CDCl_3$ or DMSO-d_6. HRMS analyses were performed on a Thermo Scientific Dionex UltiMate 3000 HPLC system with a Phenomenex Kinetex C18 column (2.1 × 150 mm, 2.6 μm) at 35 °C and equipped with a diode array detector. The samples were eluted over a gradient of solution A (0.1% formic acid in water) versus solution B (0.1% formic acid in ACN). This system was connected to a Bruker micrOTOF-Q II mass spectrometer (ESI ionization) calibrated internally with sodium formate. The purity of all the final compounds was found to be >97%, as determined by NMR and HPLC analyses.

Compound ***6***. GCLE (**4**, 1.0 g, 2.1 mmol) and NaI (314 mg, 2.1 mmol) were stirred in DMF (10 mL) for 30 min at room temperature. Then, mercaptoacetophenone (479 mg, 3.15 mmol) and sodium bicarbonate (200 mg, 2.38 mmol) were added successively, and the mixture was stirred overnight. The reaction mixture was then partitioned between water and DCM, followed by washing the organic layer with brine (3 × 20 mL). The concentration of the organic layer and purification of the residue on silica using ethyl acetate and the DCM mixture as the eluent furnished **5** as a pale-yellow solid (854 mg, 68%). ^{1}H NMR (400 MHz, $CDCl_3$): δ 7.89 (d, *J* = 8.3 Hz, aromatic H, 1H), 7.58 (t, *J* = 8.0 Hz, aromatic H, 1H), 7.45 (t, *J* = 8.0 Hz, aromatic H, 2H), 7.37−7.25 (m, aromatic H, 7H), 6.85 (dd, *J* = 8.6 Hz, *J* = 1.8 Hz, aromatic H, 2H), 5.99 (d, *J* = 9.2 Hz, 1H), 5.77 (m, β-lactam C−H, 1H), 5.14 (s, benzyloxy CH_2, 2H), 4.90 (d, *J* = 4.9 Hz, 1H), 3.99−3.45 (m, aliphatic H, 11H), ^{13}C NMR (101 MHz, DMSO-d_6): δ 194.41, 171.14, 164.50, 161.52, 159.83, 135.37, 133.72, 133.46, 130.67, 129.40, 129.10, 128.69, 128.53, 128.49, 127.64, 126.78, 124.58, 113.91, 67.93, 59.03, 57.74, 55.23, 43.26, 37.81, 33.81, 27.72. HRMS (ESI): $[M + H]^+$ calcd, 603.1624; found, 603.1620. To **5** (600 mg, 1.0 mmol) was added TFA/anisole (15 mL/3 mL), and the mixture was stirred at 0 °C for 1 h. It was then concentrated under vacuum, and the residue was precipitated by a 1:1 mixture of diethyl ether and petroleum ether. The solid was isolated by centrifugation and purified by reversed-phase prep-HPLC using a C18 column and an optimal gradient of buffer A (H_2O 95%, ACN 5%, and TFA 0.1%) versus buffer B (ACN 95%, H_2O 5%, and TFA 0.1%) to afford **6** (51 mg, 35%, based on the purification of ∼100 mg of the crude product by prep-HPLC). ^{1}H NMR (400 MHz, $CDCl_3$): δ 7.85 (d, *J* = 7.3 Hz, aromatic H, 1H), 7.53−7.22 (m, aromatic H, 8H), 6.50 (d, *J* = 8.8 Hz, 1H), 5.72 (dd, *J* = 8.9 Hz, *J* = 4.7 Hz, β-lactam C−H, 1H), 4.90 (d, *J* = 4.7 Hz, β-lactam C−H, 1H), 3.97−3.44 (m, aliphatic H, 8H), ^{13}C NMR (101 MHz, DMSO-d_6): δ 195.06, 171.36, 165.01, 163.45, 136.24, 135.91, 133.78, 129.44, 129.15, 128.79, 128.63, 127.36, 126.90, 125.49, 59.37, 58.22, 42.03, 38.20, 33.70, 27.45. HRMS (ESI): $[M - H]^-$ calcd, 481.0897; found, 481.0863.

General Procedure for the Synthesis of Compounds ***8***−***13***. To a solution of $BF_3{\cdot}OEt_2$ (2.6 mL, 21.3 mmol, 3.0 equiv) in ACN (10 mL) were added the corresponding thiols (10.7 mmol, 1.5 equiv) and 7-ACA (1.9 g, 7.1 mmol, 1.0 equiv.) successively. The mixture was stirred at 45−50° for 2 h, after which it was diluted with water and pH was adjusted to 4 by adding 28% ammonium hydroxide solution. The precipitate was filtered off and washed with cold water and acetone. The crude product (1.0 g) was added to a mixture of saturated bicarbonate solution (6 mL) and acetone (9 mL). Then, phenylacetyl chloride (2.0 equiv) was added dropwise and the mixture was stirred overnight at room temperature. Diluting the mixture with water followed by acidification to pH 2.0 using 1.0 M HCl resulted in a white solid, which was filtered off and washed with minimum water and ether. The crude material was purified by reversed-phase prep-HPLC using a C18 column and an optimal gradient of buffer A (H_2O 95%, ACN 5%, and TFA 0.1%) versus buffer B (ACN 95%, H_2O 5%, and TFA 0.1%). The quantities and yields below are reported based on the purification of 100 mg of the crude product by prep-HPLC.

Compound ***8***. 40 mg (26%, over two steps). ^{1}H NMR (400 MHz, DMSO-d_6): diastereomeric mixture δ 9.07 (apparent t, 1.8 H), 7.44−7.21 (m, aromatic H, 9H), 5.61 (m, β-lactam C−H, 1.8H), 5.04 (d, *J* = 4.8 Hz, β-lactam C−H, 0.8H), 4.88 (d, *J* = 4.7 Hz, β-lactam C−H, 1H), 4.65 (apparent d, aliphatic C−H, 1.8H), 3.69−3.32 (m, aliphatic CH_2, 10.8H), ^{13}C NMR (101 MHz, DMSO-d_6): δ 172.05, 171.98, 171.45, 171.43, 164.99, 163.52, 163.48, 137.83, 137.54, 136.29, 129.51, 129.05, 128.94, 128.89, 128.76, 128.71, 128.31, 127.24, 126.97, 125.65, 125.60, 59.38, 58.16, 52.63, 52.60, 42.06, 34.12, 33.76, 27.51, 27.44, HRMS (ESI): $[M - H]^-$ calcd, 497.0847; found, 497.0842.

Compound ***9***. 69 mg (47%, over two steps). ^{1}H NMR (400 MHz, DMSO-d_6): δ 9.14 (d, *J* = 8.3 Hz, N−H, 1H), 7.39−7.13 (m, aromatic H, 10H), 5.67 (dd, *J* = 8.3, 4.7 Hz, β-lactam C−H, 1H), 5.08 (d, *J* = 4.8 Hz, β-lactam C−H, 1H), 3.90−3.47 (m, aliphatic H, 7H), 3.04 (dd, *J* = 13.7, 9.8 Hz, aliphatic H, 1H), 2.93 (dd, *J* = 13.7, 5.8 Hz, aliphatic H, 1H), ^{13}C NMR (101 MHz, DMSO-d_6): δ 172.61, 170.99, 164.66, 163.08, 138.14, 135.84, 129.03, 129.01, 128.27, 128.23, 127.45, 126.55, 126.50, 124.95, 58.96, 57.75, 48.23, 41.58, 38.16, 33.38, 26.97, HRMS (ESI): $[M - H]^-$ calcd, 511.1003; found, 511.1000.

Compound ***10***. 33 mg (43%, over two steps). ^{1}H NMR (400 MHz, DMSO-d_6): δ 9.12 (d, *J* = 8.4 Hz, N−H, 1H), 7.37−7.17 (m, aromatic H, 10H), 5.65 (dd, *J* = 8.4, 4.7 Hz, β-lactam C−H, 1H), 4.98 (d, *J* = 4.8 Hz, β-lactam C−H, 1H), 3.73−3.33 (m, aliphatic H, 7H), 3.07 (dd, *J* = 13.8, 8.6 Hz, aliphatic H, 1H), 2.89 (dd, *J* = 13.8, 7.1 Hz, aliphatic H, 1H), ^{13}C NMR (101 MHz, DMSO-d_6): δ 173.36, 171.43, 165.03, 163.48, 138.76, 136.29, 129.61, 129.50, 128.71, 128.67, 126.98, 126.62, 125.77, 59.38, 58.19, 47.85, 42.07, 37.81, 33.57, 27.10, HRMS (ESI): $[M + H]^+$ calcd, 513.1154; found, 513.1151.

Compound ***11***. 82 mg (74%, over two steps). ^{1}H NMR (400 MHz, DMSO-d_6): δ 9.13 (d, *J* = 8.3 Hz, NH, 1H), 7.35−7.22 (m, aromatic H, 5H), 5.65 (dd, *J* = 8.3 Hz, *J* = 4.7 Hz, β-lactam C−H, 1H), 5.06 (d, *J* = 4.7 Hz, β-lactam C−H, 1H), 3.79−3.47 (m, aliphatic H, 8H), ^{13}C NMR (101 MHz, DMSO-d_6): δ 171.41, 165.11, 163.62, 138.81, 136.29, 129.49, 129.34, 128.89, 128.69, 128.22, 127.37, 126.96, 125.25, 59.40, 58.36, 42.06, 35.81, 33.78, 27.44. HRMS (ESI): $[M + H]^+$ calcd, 455.1099; found, 455.1098.

Compound ***12***. 79 mg (68%, over two steps). ^{1}H NMR (400 MHz, DMSO-d_6): δ 9.15 (d, *J* = 8.3 Hz, N−H, 1H), 7.33−7.19 (m, aromatic H, 10H), 5.65 (dd, *J* = 8.4, 4.7 Hz, β-lactam C−H, 1H), 5.13 (d, *J* = 4.7, β-lactam C−H, 1H), 3.82−3.49 (m, aliphatic H, 6H), 2.85−2.65 (m, aliphatic H, 4H). ^{13}C NMR (101 MHz, DMSO-d_6): δ 171.45, 165.20, 163.73, 140.89, 136.30, 129.50, 129.29, 129.01, 128.78, 128.70, 126.97, 126.64, 125.11, 59.40, 58.51, 42.07, 36.30, 32.95, 32.44, 27.39, HRMS (ESI): $[M + H]^+$ calcd, 469.1256; found, 469.1256.

Compound ***13***. 88 mg (27%, over two steps). ^{1}H NMR (400 MHz, DMSO-d_6): δ 9.14 (d, *J* = 8.3 Hz, N−H, 1H), 7.34−7.21 (m, aromatic H, 5H), 5.65 (dd, *J* = 8.3 Hz, *J* = 4.7 Hz, β-lactam C−H, 1H), 5.11 (d, *J* = 4.8 Hz, β-lactam C−H, 1H), 3.73−3.20 (m, aliphatic H, 8H), ^{13}C NMR (101 MHz, DMSO-d_6): δ 170.55, 170.44, 164.10, 162.47, 135.31, 128.51, 127.72, 126.48, 125.99, 124.48, 58.43, 57.31, 41.10, 32.94, 32.74, 26.42. HRMS (ESI): $[M + H]^+$ calcd, 423.0685; found, 423.0702.

Compound ***15***. 7-ADCA (**14**, 2.14 g, 10 mmol) was dissolved in saturated bicarbonate solution (20 mL), to which phenylacetyl chloride (1.5 mL, 11.3 mmol) dissolved in acetone (10 mL) was added in several portions. The mixture was stirred overnight at room temperature and then acidified to pH 2.0 using 1 M HCl. The precipitate was filtered off and washed with a minimum amount of cold water. The crude was purified by reversed-phase prep-HPLC using a C18 column and an optimal gradient of buffer A (H_2O 95%, ACN 5%, TFA 0.1%) versus buffer B (ACN 95%, H_2O 5%, TFA

https://doi.org/10.1021/acs.jmedchem.1c00362
J. Med. Chem. 2021, 64, 9141−9151

0.1%). (85 mg, 75%, based on the purification of ∼100 mg of the crude product by prep-HPLC). ^{1}H NMR (400 MHz, DMSO-d_6): δ 9.09 (d, J = 8.2 Hz, NH, 1H), 7.33−7.21 (m, aromatic H, 5H), 5.60 (dd, J = 8.2 Hz, J = 4.6 Hz, β-lactam C−H, 1H), 5.03 (d, J = 4.7 Hz, β-lactam C−H, 1H), 3.61−3.35 (m, aliphatic H, 4H), 2.03 (s, methyl, 3H), ^{13}C NMR (101 MHz, DMSO-d_6): δ 171.44, 164.82, 163.98, 136.33, 130.21, 129.48, 128.68, 126.93, 123.21, 59.33, 57.56, 42.03, 29.40, 19.87. HRMS (ESI): $[M + H]^+$ calcd, 333.0909; found, 333.0917.

Enzyme Production and Purification. The procedures for the overexpression and purification of IMP-1, IMP-28, NDM-1, and VIM-2 have been described in detail in the previous publication.[12,31]

*Enzymatic Preparation of **8H** and **9H**.* Compounds **8** and **9** (2 mM each) were incubated with NDM-1 (187 nM) at room temperature in 50 mM 4-(2-hydroxyethyl)-1-piperazineethanesulfonic acid (HEPES)−NaOH, pH 7.2, supplemented with 1 μM $ZnSO_4$ and 0.01% Triton X-100. The progress of hydrolysis was monitored by LC−MS (Figure S8). After 2 h, the conversion was complete, and compounds **8H** and **9H** were separated from the enzyme by spin filtration (3 kDa filter cutoff, Amicon) at 12,000 rpm for 5 min.

Enzyme Inhibition Assay. The cephalosporin derivatives were tested for their inhibitory activity against NDM-1, VIM-2, and IMP-28 using the chromogenic substrate nitrocefin. The assay buffer was 50 mM HEPES, pH 7.2, supplemented with 1 μM $ZnSO_4$ and 0.01% Triton X-100. In brief, on a flat-bottom polystyrene 96-well microplate NDM-1 (6 nM), VIM-2 (8 nM), or IMP-28 (1 nM) was incubated with various concentrations of the test compounds for 15−60 min at 25 °C. Nitrocefin (10 μM, ∼2 × K_M) was added to the wells, and absorption at 492 nm was immediately monitored on a TECAN Spark microplate reader over 30 scan cycles. For measuring time 0 in the time-dependent IC_{50} assay, the enzyme was added last, after which the absorbance was immediately measured. The initial velocity data were used for IC_{50} curve-fitting using GraphPad Prism 7. All the compounds were tested in three independent replicates.

Determination of the Kinetic Parameters of Cephalosporin Conjugates. Hydrolysis of the cephalosporin conjugates was monitored on a Tecan Spark microplate reader using UV-transparent 96-well plates (UV-Star, Greiner). Various concentrations of the test compounds were dissolved in 50 mM HEPES−NaOH, pH 7.2, supplemented with 1 μM $ZnSO_4$ and 0.01% Triton X-100. Followed by the addition of MBLs dissolved in the same buffer, absorption at 260 nm was measured immediately over 30−40 scan cycles at 25 °C. The obtained initial velocity data were plotted against the substrate concentration, and K_M and V_{max} were determined using the Michaelis−Menten fitting model on GraphPad Prism 7.

MIC Determination and Synergy Assays. The MIC of the test compounds was determined following the guidelines published by Clinical and Laboratory Standards Institute (CLSI) and as described earlier.[11] Synergy between the cephalosporin derivatives and β-lactam antibiotics was evaluated by the following protocol: β-lactam antibiotics dissolved in MHB with the concentration corresponding to 4× MIC was added to polypropylene 96-well microplates and serially diluted (25 μL/well). Then, all three columns received a fixed concentration of the test compounds dissolved in MHB (25 μL/well). Multiple concentrations of the test compounds were evaluated in this way. Finally, bacterial suspensions grown to the OD_{600} of 0.5 were diluted 100× in MHB before adding to the plate (50 μL/well). The microplates were then covered with breathable seals and incubated overnight with shaking at 37 °C for 15−20 h. Dipicolinic acid was used as the positive control.

Stability Analysis in MHB. The solutions of the test compounds (1 mM) in MHB were incubated at 37 °C for 15 h. Then, 100 μL of the MHB solution was precipitated by adding to ACN (200 μL) supplemented with 2 mM benzocaine, vortexed, and centrifuged (12,000 rpm, 5 min). The supernatant was analyzed by reversed-phase analytical HPLC using a C_{18} column and an optimal gradient of buffer A (H_2O 95%, ACN 5%, and TFA 0.1%) versus buffer B (ACN 95%, H_2O 5%, and TFA 0.1%). The detector wavelength was set at 254 nm.

Isothermal Titration Calorimetry. The ITC titrations were performed on a PEAQ-ITC calorimeter (Malvern). All the test compounds and zinc sulfate were dissolved in 20 mM Tris−HCl buffer (pH 7.0). The experiments consisted of titrating 2 mM zinc sulfate through 19 × 2.0 μL aliquots (except the first aliquot which was 0.4 μL) into 200 μM solutions of the cephalosporin conjugates incubated with NDM-1 (187 nM) for 2 h at room temperature. The experiments were performed at 25 °C with 150 s interval between titrations, and reference power was set at 10.0 μcal/s. The data were analyzed using Microcal PEAQ-ITC analysis software. In separate experiments, upon the titration of zinc sulfate into the solutions of cephalosporin conjugates or NDM-1, no binding interaction was observed.

NMR-Based Monitoring of the Enzymatic Hydrolysis. The cephalosporin conjugates were dissolved in DMSO-d_6 and diluted in deuterated PBS (pH 7.4) or deuterated 50 mM HEPES (pH 7.4), each supplemented with 1 μM $ZnSO_4$. IMP-28 was added to the solution, and the final concentration of the enzyme, test compounds, and DMSO were 320 nM, 1 mg/mL, and 1%, respectively. Following incubation at 25 °C, the ^{1}H NMR spectra were measured on a Bruker 400 MHz spectrometer at various time points.

LCMS-Based Monitoring of the Enzymatic Hydrolysis. The cephalosporin conjugates were dissolved in 50 mM HEPES buffer (pH 7.2) supplemented with 1 μM $ZnSO_4$ and 0.01% Triton X-100. IMP-28 was added to the solution, and the final concentration of the enzyme, test compounds, and DMSO were 320 nM, 1 mg/mL, and 1% respectively. Following incubation at 25 °C and at different time points, the solution was diluted in ACN (1:2 v/v) and centrifuged at 12,000 rpm for 5 min. The supernatant was analyzed on an LCMS-8040 triple-quadrupole liquid chromatograph mass spectrometer (LC−MS/MS, Shimadzu) using a C18 column (3 μm, 3.0 × 150 mm, Shimadzu) and a gradient of 5−100% pure ACN against 0.1% formic acid.

In Silico Studies. All computational modeling was performed in the Schrodinger Suite version 2019-4.[32] Figures were generated using PyMOL. 3D coordinates of the ligands were generated using LigPrep[33] with the OPLS3e forcefield.[34] Protein structures for IMP-1 (PDB ID: 1dd6)[19] and NDM-1 (PDB ID: 4RL2)[16] were prepared using the Protein Preparation Wizard.[35,36] Thereafter, compounds were docked using GLIDE-SP.[37] A maximum common substructure constraint for all product compounds was used, which was derived from cephalexin coordinates in PDB ID 4RL2. The substrate compounds were docked without using constraints. The best pose was maintained according to GLIDE docking score and visual inspection of the poses. MD simulations were performed using Desmond[38] in the Schrodinger Suite using the standard protocol for system setup, using the OPLS3 forcefield.[34] Three replicate-independent 10 ns simulations were run for each of the reported protein−ligand systems.

■ ASSOCIATED CONTENT

Supporting Information

The Supporting Information is available free of charge at https://pubs.acs.org/doi/10.1021/acs.jmedchem.1c00362.

Molecular formula strings, analytical-spectral data including ^{1}H NMR, ^{13}C NMR, and HPLC traces, IC_{50} curves, stability data, enzymatic degradation monitored by ^{1}H NMR and LCMS, docking figures, and PDB coordinates for compounds **8** and **8H** docked into IMP-1 and NDM-1 active sites (PDF)

Molecular formula strings (CSV)

PDB coordinates (ZIP)

■ AUTHOR INFORMATION

Corresponding Author

Nathaniel I. Martin − *Biological Chemistry Group, Institute of Biology Leiden, Leiden University, 2333 BE Leiden, The Netherlands;* orcid.org/0000-0001-8246-3006; Email: n.i.martin@biology.leidenuniv.nl

https://doi.org/10.1021/acs.jmedchem.1c00362
J. Med. Chem. 2021, 64, 9141−9151

Authors

Kamaleddin H. M. E. Tehrani − *Biological Chemistry Group, Institute of Biology Leiden, Leiden University, 2333 BE Leiden, The Netherlands*

Nicola Wade − *Biological Chemistry Group, Institute of Biology Leiden, Leiden University, 2333 BE Leiden, The Netherlands*

Vida Mashayekhi − *Division of Cell Biology, Department of Biology, Faculty of Science, Utrecht University, 3584 CH Utrecht, The Netherlands*

Nora C. Brüchle − *Biological Chemistry Group, Institute of Biology Leiden, Leiden University, 2333 BE Leiden, The Netherlands*

Willem Jespers − *Department of Cell and Molecular Biology, Biomedical Center, Uppsala University, SE-751 24 Uppsala, Sweden; Division of Drug Discovery & Safety, Leiden Academic Centre for Drug Research, Leiden University, 2333 CC Leiden, The Netherlands*

Koen Voskuil − *Biological Chemistry Group, Institute of Biology Leiden, Leiden University, 2333 BE Leiden, The Netherlands*

Diego Pesce − *Laboratory of Genetics, Wageningen University and Research, 6700 AA Wageningen, The Netherlands; Department of Evolutionary Biology and Environmental Studies, University of Zurich, 8057 Zurich, Switzerland*

Matthijs J. van Haren − *Biological Chemistry Group, Institute of Biology Leiden, Leiden University, 2333 BE Leiden, The Netherlands*

Gerard J. P. van Westen − *Division of Drug Discovery & Safety, Leiden Academic Centre for Drug Research, Leiden University, 2333 CC Leiden, The Netherlands;* orcid.org/0000-0003-0717-1817

Complete contact information is available at: https://pubs.acs.org/10.1021/acs.jmedchem.1c00362

Notes

The authors declare no competing financial interest.

■ ACKNOWLEDGMENTS

Funding was provided by the European Research Council (ERC consolidator grant to NIM, grant agreement no. 725523).

■ ABBREVIATIONS

7-ACA, 7-aminocephalosporanic acid; 7-ADCA, 7-aminodesacetoxycephalosporanic acid; DPA, dipicolinic acid; IMP, imipenemase; ITC, isothermal titration calorimetry; NDM, New Delhi metallo-β-lactamase; MCS, maximum common substructure; MBL, metallo-β-lactamase; MHB, Mueller−Hinton broth; VIM, Verona integron-encoded metallo-β-lactamase

■ REFERENCES

(1) Spencer, J.; Read, J.; Sessions, R. B.; Howell, S.; Blackburn, G. M.; Gamblin, S. J. Antibiotic recognition by binuclear metallo-β-lactamases revealed by X-ray crystallography. *J. Am. Chem. Soc.* **2005**, *127*, 14439−14444.

(2) King, D. T.; Worrall, L. J.; Gruninger, R.; Strynadka, N. C. J. New Delhi metallo-β-lactamase: structural insights into β-Lactam recognition and inhibition. *J. Am. Chem. Soc.* **2012**, *134*, 11362−11365.

(3) Drawz, S. M.; Bonomo, R. A. Three decades of beta-lactamase inhibitors. *Clin. Microbiol. Rev.* **2010**, *23*, 160−201.

(4) Bonomo, R. A.; Burd, E. M.; Conly, J.; Limbago, B. M.; Poirel, L.; Segre, J. A.; Westblade, L. F. Carbapenemase-producing organisms: a global scourge. *Clin. Infect. Dis.* **2017**, *66*, 1290−1297.

(5) McGeary, R. P.; Tan, D. T.; Schenk, G. Progress toward inhibitors of metallo-β-lactamases. *Future Med. Chem.* **2017**, *9*, 673−691.

(6) Groundwater, P. W.; Xu, S.; Lai, F.; Váradi, L.; Tan, J.; Perry, J. D.; Hibbs, D. E. New Delhi metallo-β-lactamase-1: structure, inhibitors and detection of producers. *Future Med. Chem.* **2016**, *8*, 993−1012.

(7) Tehrani, K. H. M. E.; Martin, N. I. β-Lactam/β-lactamase inhibitor combinations: an update. *Medchemcomm* **2018**, *9*, 1439−1456.

(8) Fast, W.; Sutton, L. D. Metallo-β-lactamase: inhibitors and reporter substrates. *Biochim. Biophys. Acta, Proteins Proteomics* **2013**, *1834*, 1648−1659.

(9) Ju, L.-C.; Cheng, Z.; Fast, W.; Bonomo, R. A.; Crowder, M. W. The continuing Challenge of metallo-β-lactamase inhibition: mechanism matters. *Trends Pharmacol. Sci.* **2018**, *39*, 635−647.

(10) Rotondo, C. M.; Wright, G. D. Inhibitors of metallo-β-lactamases. *Curr. Opin. Microbiol.* **2017**, *39*, 96−105.

(11) Tehrani, K. H. M. E.; Martin, N. I. Thiol-containing metallo-β-lactamase inhibitors resensitize resistant gram-negative bacteria to meropenem. *ACS Infect. Dis.* **2017**, *3*, 711−717.

(12) van Haren, M. J.; Tehrani, K. H. M. E.; Kotsogianni, I.; Wade, N.; Brüchle, N.; Mashayekhi, V.; Martin, N. I. Cephalosporin prodrug inhibitors overcome metallo-β-lactamase driven antibiotic resistance. *Chem.—Eur. J.* **2020**, *27*, 3806−3811.

(13) Strijtveen, B.; Kellogg, R. M. Synthesis of (racemization prone) optically active thiols by SN2 substitution using cesium thiocarboxylates. *J. Org. Chem.* **1986**, *51*, 3664.

(14) Pérez-Llarena, F. J.; Fernández, A.; Zamorano, L.; Kerff, F.; Beceiro, A.; Aracil, B.; Cercenado, E.; Miro, E.; Oliver, A.; Oteo, J.; Navarro, F.; Bou, G. Characterization of a novel IMP-28 metallo-β-lactamase from a Spanish Klebsiella oxytoca clinical isolate. *Antimicrob. Agents Chemother.* **2012**, *56*, 4540−4543.

(15) Hanessian, S.; Wang, J. Design and synthesis of a cephalosporin−carboplatinum prodrug activatable by a β-lactamase. *Can. J. Chem.* **1993**, *71*, 896−906.

(16) Feng, H.; Ding, J.; Zhu, D.; Liu, X.; Xu, X.; Zhang, Y.; Zang, S.; Wang, D.-C.; Liu, W. Structural and mechanistic insights into NDM-1 catalyzed hydrolysis of cephalosporins. *J. Am. Chem. Soc.* **2014**, *136*, 14694−14697.

(17) Evans, L. E.; Krishna, A.; Ma, Y.; Webb, T. E.; Marshall, D. C.; Tooke, C. L.; Spencer, J.; Clarke, T. B.; Armstrong, A.; Edwards, A. M. Exploitation of antibiotic resistance as a novel drug target: development of a β-lactamase-activated antibacterial prodrug. *J. Med. Chem.* **2019**, *62*, 4411−4425.

(18) Jackson, A. C.; Zaengle-Barone, J. M.; Puccio, E. A.; Franz, K. J. A Cephalosporin prochelator inhibits New Delhi metallo-β-lactamase 1 without removing zinc. *ACS Infect. Dis.* **2020**, *6*, 1264−1272.

(19) Concha, N. O.; Janson, C. A.; Rowling, P.; Pearson, S.; Cheever, C. A.; Clarke, B. P.; Lewis, C.; Galleni, M.; Frère, J.-M.; Payne, D. J.; Bateson, J. H.; Abdel-Meguid, S. S. Crystal structure of the IMP-1 metallo-β-lactamase from Pseudomonas Aeruginosa and its complex with a mercaptocarboxylate inhibitor: binding determinants of a potent, broad-spectrum inhibitor. *Biochemistry* **2000**, *39*, 4288−4298.

(20) Liu, B.; Trout, R. E. L.; Chu, G.-H.; McGarry, D.; Jackson, R. W.; Hamrick, J. C.; Daigle, D. M.; Cusick, S. M.; Pozzi, C.; De Luca, F.; Benvenuti, M.; Mangani, S.; Docquier, J.-D.; Weiss, W. J.; Pevear, D. C.; Xerri, L.; Burns, C. J. Discovery of taniborbactam (VNRX-5133): a broad-spectrum serine- and metallo-β-lactamase inhibitor for carbapenem-resistant bacterial infections. *J. Med. Chem.* **2020**, *63*, 2789−2801.

(21) Brem, J.; Rydzik, A. M.; Mcdonough, M. A.; Schofield, C. J.; Morrison, A.; Hewitt, J.; Pannifer, A.; Jones, P. Inhibitors of metallo-beta-lactamases. WO 2017093727 A1, 2017.

(22) Everett, M.; Sprynski, N.; Coelho, A.; Castandet, J.; Bayet, M.; Bougnon, J.; Lozano, C.; Davies, D. T.; Leiris, S.; Zalacain, M.; Morrissey, I.; Magnet, S.; Holden, K.; Warn, P.; De Luca, F.; Docquier, J. D.; Lemonnier, M. Discovery of a novel metallo-β-lactamase inhibitor that potentiates meropenem activity against carbapenem-resistant Enterobacteriaceae. *Antimicrob. Agents Chemother.* **2018**, *62*, No. e00074.
(23) Leiris, S.; Coelho, A.; Castandet, J.; Bayet, M.; Lozano, C.; Bougnon, J.; Bousquet, J.; Everett, M.; Lemonnier, M.; Sprynski, N.; Zalacain, M.; Pallin, T. D.; Cramp, M. C.; Jennings, N.; Raphy, G.; Jones, M. W.; Pattipati, R.; Shankar, B.; Sivasubrahmanyam, R.; Soodhagani, A. K.; Juventhala, R. R.; Pottabathini, N.; Pothukanuri, S.; Benvenuti, M.; Pozzi, C.; Mangani, S.; De Luca, F.; Cerboni, G.; Docquier, J.-D.; Davies, D. T. SAR studies leading to the identification of a novel series of metallo-β-lactamase inhibitors for the treatment of carbapenem-resistant Enterobacteriaceae infections that display efficacy in an animal infection model. *ACS Infect. Dis.* **2019**, *5*, 131−140.
(24) Thomas, C. A.; Cheng, Z.; Yang, K.; Hellwarth, E.; Yurkiewicz, C. J.; Baxter, F. M.; Fullington, S. A.; Klinsky, S. A.; Otto, J. L.; Chen, A. Y.; Cohen, S. M.; Crowder, M. W. Probing the mechanisms of inhibition for various inhibitors of metallo-β-lactamases VIM-2 and NDM-1. *J. Inorg. Biochem.* **2020**, *210*, 111123.
(25) Wade, N.; Tehrani, K. H. M. E.; Brüchle, N. C.; Haren, M. J.; Mashayekhi, V.; Martin, N. I. Mechanistic Investigations of Metallo-β-Lactamase Inhibitors: Strong zinc binding is not required for potent enzyme inhibition. *ChemMedChem* **2021**, *16*, 1651−1659.
(26) Cahill, S. T.; Cain, R.; Wang, D. Y.; Lohans, C. T.; Wareham, D. W.; Oswin, H. P.; Mohammed, J.; Spencer, J.; Fishwick, C. W. G.; McDonough, M. A.; Schofield, C. J.; Brem, J. Cyclic boronates inhibit all classes of β-lactamases. *Antimicrob. Agents Chemother.* **2017**, *61*, No. e02260.
(27) Garau, G.; Bebrone, C.; Anne, C.; Galleni, M.; Frère, J.-M.; Dideberg, O. A metallo-β-lactamase enzyme in action: crystal structures of the monozinc carbapenemase CphA and its complex with biapenem. *J. Mol. Biol.* **2005**, *345*, 785−795.
(28) Ullah, J. H.; Walsh, T. R.; Taylor, I. A.; Emery, D. C.; Verma, C. S.; Gamblin, S. J.; Spencer, J. The Crystal structure of the L1 metallo-beta-lactamase from Stenotrophomonas maltophilia at 1.7 A resolution. *J. Mol. Biol.* **1998**, *284*, 125−136.
(29) Leiros, H.-K. S.; Borra, P. S.; Brandsdal, B. O.; Edvardsen, K. S. W.; Spencer, J.; Walsh, T. R.; Samuelsen, Ø. Crystal structure of the mobile metallo-beta-lactamase AIM-1 from Pseudomonas aeruginosa: insights into antibiotic binding and the role of Gln157. *Antimicrob. Agents Chemother.* **2012**, *56*, 4341−4353.
(30) Keltjens, R.; Vadivel, S. K.; De Vroom, E.; Klunder, A. J. H.; Zwanenburg, B. A New Convenient synthesis of 3-carboxycephems starting from 7-aminocephalosporanic acid (7-ACA). *Eur. J. Org. Chem.* **2001**, *2001*, 2529−2534.
(31) Tehrani, K. H. M. E.; Brüchle, N. C.; Wade, N.; Mashayekhi, V.; Pesce, D.; van Haren, M. J.; Martin, N. I. Small molecule carboxylates inhibit metallo-β-lactamases and resensitize carbapenem-resistant bacteria to meropenem. *ACS Infect. Dis.* **2020**, *6*, 1366−1371.
(32) *Schrödinger Release 2019-4*: Maestro, Schrödinger, LLC, New York, NY, 2019.
(33) *Schrödinger Release 2019-4*: LigPrep, Schrödinger, LLC, New York, NY, 2019.
(34) Roos, K.; Wu, C.; Damm, W.; Reboul, M.; Stevenson, J. M.; Lu, C.; Dahlgren, M. K.; Mondal, S.; Chen, W.; Wang, L.; Abel, R.; Friesner, R. A.; Harder, E. D. OPLS3e: extending force field coverage for drug-like small molecules. *J. Chem. Theory Comput.* **2019**, *15*, 1863−1874.
(35) Madhavi Sastry, G.; Adzhigirey, M.; Day, T.; Annabhimoju, R.; Sherman, W. Protein and ligand preparation: parameters, protocols, and influence on virtual screening enrichments. *J. Comput.-Aided Mol. Des.* **2013**, *27*, 221−234.
(36) Schrödinger Release 2020-4: Protein Preparation Wizard; Epik, Schrödinger, LLC, New York, NY, 2016; Impact, Schrödinger, LLC, New York, NY, 2016; Prime, Schrödinger, LLC, New York, NY, 2020.
(37) Friesner, R. A.; Banks, J. L.; Murphy, R. B.; Halgren, T. A.; Klicic, J. J.; Mainz, D. T.; Repasky, M. P.; Knoll, E. H.; Shelley, M.; Perry, J. K.; Shaw, D. E.; Francis, P.; Shenkin, P. S. Glide: a new approach for rapid, accurate docking and scoring. 1. method and assessment of docking accuracy. *J. Med. Chem.* **2004**, *47*, 1739−1749.
(38) *SC'06: Proceedings of the 2006 ACM/IEEE Conference on Supercomputing*; Association for Computing Machinery: New York, NY, USA, 2006.

https://doi.org/10.1021/acs.jmedchem.1c00362
J. Med. Chem. 2021, 64, 9141−9151